*Geophysical Prospecting*

Geophysical Prospecting

ORIGINAL ARTICLE OPEN ACCESS

# Application of Marchenko-Based Isolation to a Land S-Wave Seismic Dataset

Faezeh Shirmohammadi[1,2] | Deyan Draganov[1] | Johno van IJsseldijk[1] | Ranajit Ghose[1] | Jan Thorbecke[1] | Eric Verschuur[1] | Kees Wapenaar[1]

[1]Department of Geoscience and Engineering, Delft University of Technology, Delft, The Netherlands | [2]Fugro Innovation & Technology B.V., Nootdorp, The Netherlands

**Correspondence:** Deyan Draganov (D.S.Draganov@tudelft.nl)

**Received:** 25 October 2024 | **Accepted:** 24 July 2025

**Funding**: This research is funded by NWO Science domain (NWO-ENW), project DEEP.NL.2018.048, and the reflection dataset was acquired by funding from the European Research Council under the European Union's Horizon 2020 research and innovation programme (Grant Agreement No. 742703) and OYO Corporation, Japan: OYO-TUD Research Collaboration (Project code C25B74).

**Keywords:** data processing | imaging | seismics

## ABSTRACT

The overburden structures often can distort the responses of the target region in seismic data, especially in land datasets. Ideally, all effects of the overburden and underburden structures should be removed, leaving only the responses of the target region. This can be achieved using the Marchenko method. The Marchenko method is capable of estimating Green's functions between the surface of the Earth and arbitrary locations in the subsurface. These Green's functions can then be used to redatum wavefields to a level in the subsurface. As a result, the Marchenko method enables the isolation of the response of a specific layer or package of layers, free from the influence of the overburden and underburden. In this study, we apply the Marchenko-based isolation technique to land S-wave seismic data acquired in the Groningen province, the Netherlands. We apply the technique for combined removal of the overburden and underburden, which leaves the isolated response of the target region, which is selected between 30 and 270 m depth. Our results indicate that this approach enhances the resolution of reflection data. These enhanced reflections can be utilised for imaging and monitoring applications.

## 1 | Introduction

In seismic data, the focus generally rests on target zones in the Earth's subsurface, for example, for $CO_2$ and $H_2$ storage. However, the responses from these target zones are typically distorted due to interference from overburden and underburden structures, particularly in land seismic datasets. Therefore, it is essential to eliminate the effects of the overburden and underburden, which can be achieved using the Marchenko method.

The Marchenko method – a data-driven method – provides a tool for extracting information about the subsurface properties of the Earth. The Marchenko method retrieves Green's functions in the subsurface from seismic reflection data at the surface. These Green's functions can be used to redatum wavefields from the surface to arbitrary locations in the subsurface; a virtual source or receiver can be created at any point inside the medium of interest. This method employs reflection data from sources and receivers at the surface and an estimation of the first arrival, from the surface to a point in the subsurface to which we want to redatum. The first arrival can be estimated using a smooth (macro) velocity model (Slob et al. 2014; Wapenaar et al. 2014a). Such a model could be obtained from the standard reflection processing, for example, from the stacking-velocities model and

can thus be complex or simple, depending on the data itself. The required input for the Marchenko method is similar to that for traditional redatuming techniques. However, the information needed to deal with internal multiples is derived entirely from the reflection dataset, rather than relying on a detailed subsurface model as needed by the traditional redatuming methods (e.g., Mulder 2005; Malcolm et al. 2007). Compared to redatuming methods based on seismic interferometry, the Marchenko method allows for wavefield redatuming to locations in the subsurface where no physical receivers (or sources) were present, rather than requiring physical receivers (or sources) at the depth level which is targeted with the redatuming (e.g., Schuster et al. 2004; Bakulin and Calvert 2006; Shirmohammadi et al. 2021).

In recent years, there has been significant progress in developing the Marchenko method and extending its applicability, for instance, for isolating the response of a specific subsurface layer without interference from the overburden and/or underburden. For an easier comparison with the original reflection data, the result of the Marchenko method can be extrapolated back to the surface (van der Neut and Wapenaar 2016; Meles et al. 2016). This application results in a reflection response with sources and receivers at the surface with fewer internal multiples from the overburden, and it is significantly less sensitive to the chosen velocity model. This allows for more accurate characterisation of the properties of the target layer and can be particularly useful in target-oriented imaging and monitoring. Wapenaar and van IJsseldijk (2021) introduced the Marchenko-based isolation to identify the reservoir response from a seismic reflection survey by applying a two-step approach for removing the overburden and underburden interferences. Van IJsseldijk et al. (2023) showed that this application effectively isolates the target response, which can then be used to extract more precisely the local time-lapse changes in a reservoir. The Marchenko method for isolating a target response has been successfully applied to marine time-lapse datasets of the Troll Field for monitoring reservoir changes (van IJsseldijk et al.2024).

As with any other method, the Marchenko method has some limitations. For its standard application, evanescent waves are ignored, the medium of interest is assumed to be lossless, and it is sensitive to time and amplitude inaccuracies in the reflection response. These facts can pose challenges, particularly when applied to noisy field data. Nevertheless, the method has been successfully applied to several marine field datasets for imaging and monitoring (Ravasi et al. 2016; Jia et al. 2018; Staring et al. 2018; Mildner et al. 2019; Zhang and Slob 2020; van IJsseldijk et al. 2024). In spite of these advances, applications of the Marchenko method to land seismic data remain limited and relatively more problematic not only because a reflection dataset free of surface waves and surface-related multiples is required but also because the recorded data are inherently elastic (Reinicke et al. 2020).

Here, we aim to apply the Marchenko-based isolation method to an SH-wave seismic dataset acquired close to the town of Scheemda in the Groningen province, the Netherlands, to isolate the target response, removing the overburden and underburden. The province of Groningen has been experiencing induced seismicity due to gas production since 1963 (Muntendam-Bos et al. 2022). Down to 800 m depth, the subsurface in Groningen comprises a sequence of sediments, mainly composed of sand and clay (Kruiver et al. 2017). Achieving an accurate depiction of the geometry and characteristics of these layers is crucial for precise earthquake studies. However, as known from cone penetration testing (CPT) data, the first 30 m of this site consists of alternating layers capable of generating strong internal multiples, which interfere with the response of all layers in the subsurface. Additionally, the deeper layers may generate arrivals that interfere with multiple reflections from the shallower layers. We acquired a reflection dataset specifically in this region to showcase the effectiveness of the Marchenko-based isolation method on land data and to enhance the visualisation of the reflection dataset in this region.

In the following section, we first review Marchenko-based isolation. Next, we describe the seismic acquisition parameters and the steps for preparing the input data for the Marchenko application. Finally, we discuss the results and how this study can contribute to future utilisation of the method, particularly for land-based applications.

## 2 | Method

Using the Marchenko method, we aim to isolate responses from a target layer by eliminating undesired events, including primaries and multiples, originating from both the overburden and underburden. To achieve this, the medium is divided into three units: overburden $\langle a \rangle$, target zone $\langle b \rangle$ and underburden $\langle c \rangle$, as shown in Figure 1. In the first step, the extrapolated Green's functions are determined with a focal level situated between the overburden $\langle a \rangle$ and the target zone $\langle b \rangle$ by using the Marchenko focusing functions.

Next, the overburden is removed, and the reflection response of the combined target zone $\langle b \rangle$ and underburden $\langle c \rangle$ is retrieved by applying seismic interferometry (SI) by multidimensional deconvolution (MDD; Broggini et al. 2014) with the extrapolated Green's functions. In the following step, the newly obtained reflection response is used to retrieve the extrapolated Marchenko focusing functions with a focal level situated between the target zone $\langle b \rangle$ and the underburden $\langle c \rangle$. These retrieved Marchenko focusing functions are then used to remove the underburden using SI by MDD, effectively isolating the response of the target layer $\langle b \rangle$.

In the following subsections, we present the representations of Green's functions and then demonstrate how to isolate the responses of the target layer by eliminating the effects of the overburden and underburden.

### 2.1 | Green's Functions Representation

The Marchenko method relies on two equations that relate the Green's functions ($G^{-,\pm}$) and the focusing functions ($f_1^{\pm}$), derived from the one-way reciprocity theorems of the correlation and convolution types (Slob et al. 2014; Wapenaar et al. 2014b, 2021). The left superscript ($-$) of the Green's function denotes that the wavefield is upgoing at the receiver position (at the acquisition surface) and the superscript ($\pm$) denotes a down- or up-going direction from the (virtual) source position (at the

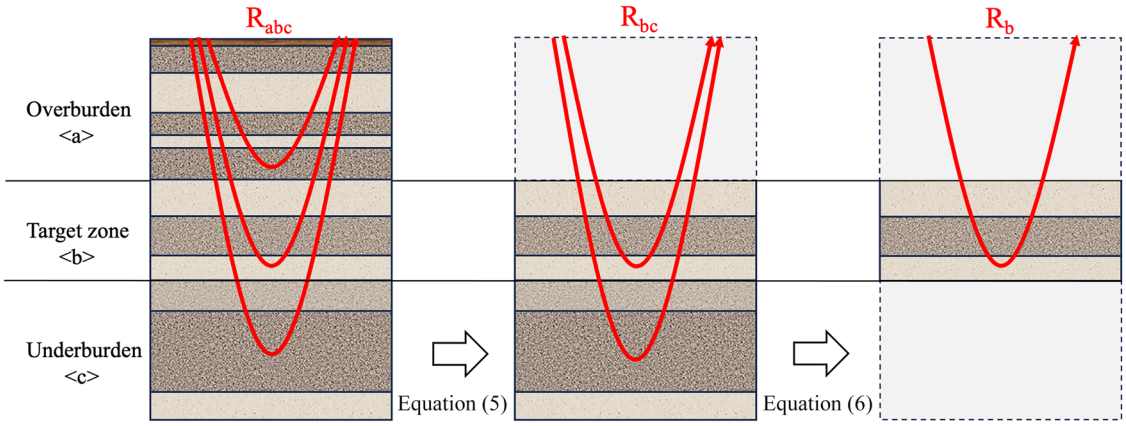


**Figure 1** | Visual representation of the concept of Marchenko-based isolation. The medium is segmented into three units: overburden $\langle a \rangle$, target zone $\langle b \rangle$ and underburden $\langle c \rangle$. The initial step involves the removal of the overburden from the recorded response, as outlined in Equation (5). Following this, the response of the underburden is removed using Equation (6). The red rays represent some of the interactions within the overburden, target layers and underburden, which can be primaries or internal multiples (adapted from van IJsseldijk et al. 2024).

focal depth). The superscript $(\pm)$ of the focusing function denotes downward and upward propagation at the acquisition surface. Focusing functions are operators specifically designed to focus the wavefield at a particular location within the subsurface. These functions are defined in a truncated medium, which matches the actual medium above the chosen focal level and is homogeneous below it. In the actual medium, focusing functions enable the wavefield to converge at the focal point, thereby facilitating the creation of a virtual source that generates Green's functions between the focal depth and the surface. The Marchenko method only requires the reflection responses at the surface and the first arrivals between the surface and the focal depth, which can be estimated using a smooth velocity model of the subsurface.

Meles et al. (2016) and van der Neut and Wapenaar (2016) proposed extrapolating the virtual sources and receivers, obtained through Marchenko redatuming, back to the surface. This approach ensures that the travel times of events in the processed response remain consistent with the corresponding events in the original reflection data, allowing for easier comparison of results before and after applying the Marchenko method. Both the focusing and the Green's functions are extrapolated using the direct arrival of the transmission response ($T_d$) from the focal depth to the surface (van der Neut and Wapenaar 2016), ensuring that the coordinates of all functions are located at the acquisition surface, $S_0$. These extrapolated focusing functions ($v^{\pm}$) and the extrapolated Green's functions $U^{-,\pm}$ are defined as follows (van IJsseldijk et al. 2023):

$$v^{\pm}(\mathbf{x}_R, \mathbf{x}'_S, t) = \int_{S_F} f_1^{\pm}(\mathbf{x}_R, \mathbf{x}_F, t) * T_d(\mathbf{x}_F, \mathbf{x}'_S, t) d\mathbf{x}_F, \quad (1)$$

$$U^{-,\pm}(\mathbf{x}_R, \mathbf{x}'_S, \pm t) = \int_{S_F} G^{-,\pm}(\mathbf{x}_R, \mathbf{x}_F, \pm t) * T_d(\mathbf{x}_F, \mathbf{x}'_S, t) d\mathbf{x}_F. \quad (2)$$

Here, $\mathbf{x}_F$ is the coordinate at the focal depth $S_F$ and $\mathbf{x}'_S$ is a coordinate at the acquisition surface. The symbol $*$ denotes temporal convolution. The same convolutions are applied to the coupled Marchenko representations to determine the extrapolated representations. Therefore, the retrieved wavefields from the extrapolated Marchenko method are not at the focal depth ($S_F$) but at the surface ($S_0$). The coupled Marchenko extrapolated representations are defined as (Wapenaar et al. 2021; van IJsseldijk et al. 2024):

$$U^{-,+}(\mathbf{x}_R, \mathbf{x}'_S, t) + v^{-}(\mathbf{x}_R, \mathbf{x}'_S, t) = \int_{S_0} R(\mathbf{x}_R, \mathbf{x}_S, t) * v^{+}(\mathbf{x}_S, \mathbf{x}'_S, t) d\mathbf{x}_S, \quad (3)$$

$$U^{-,-}(\mathbf{x}_R, \mathbf{x}'_S, -t) + v^{+}(\mathbf{x}_R, \mathbf{x}'_S, t) = \int_{S_0} R(\mathbf{x}_R, \mathbf{x}_S, -t) * v^{-}(\mathbf{x}_S, \mathbf{x}'_S, t) d\mathbf{x}_S, \quad (4)$$

which relate the extrapolated Green's function $U^{-,\pm}$ to the extrapolated focusing functions ($v^{\pm}$) using the reflection response $R(\mathbf{x}_R, \mathbf{x}_S, t)$ at the acquisition surface ($S_0$). Here, $\mathbf{x}_R$, $\mathbf{x}_S$ and $\mathbf{x}'_S$ describe the receiver and source positions at the surface, respectively.

Given that $R$ is known, Equations (3) and (4) involve four unknowns ($U^{-,-}$, $U^{-,+}$, $v^{-}$, and $v^{+}$). To solve these equations, a window function is applied to suppress the extrapolated Green's functions. This approach relies on the fact that the extrapolated focusing functions and Green's functions are separable in time (van der Neut and Wapenaar 2016). This causality constraint can be applied after estimating the two-way travel time between the focal depth and the surface, which can be obtained from a smooth velocity model. By restricting Equations (3) and (4) to the time interval between zero and the calculated two-way travel time, the Green's functions on the left-hand side vanish. This simplifies the system to two equations with two unknowns (the extrapolated focusing functions), which can be solved iteratively (Thorbecke et al. 2017) or through inversion (van der Neut et al. 2015). Once the focusing functions are found, the extrapolated Green's functions follow from Equations (3) and (4) without the time restriction. A detailed derivation of the Marchenko method is beyond the scope of this paper; however, a comprehensive derivation and background can be found in Wapenaar et al. (2021).

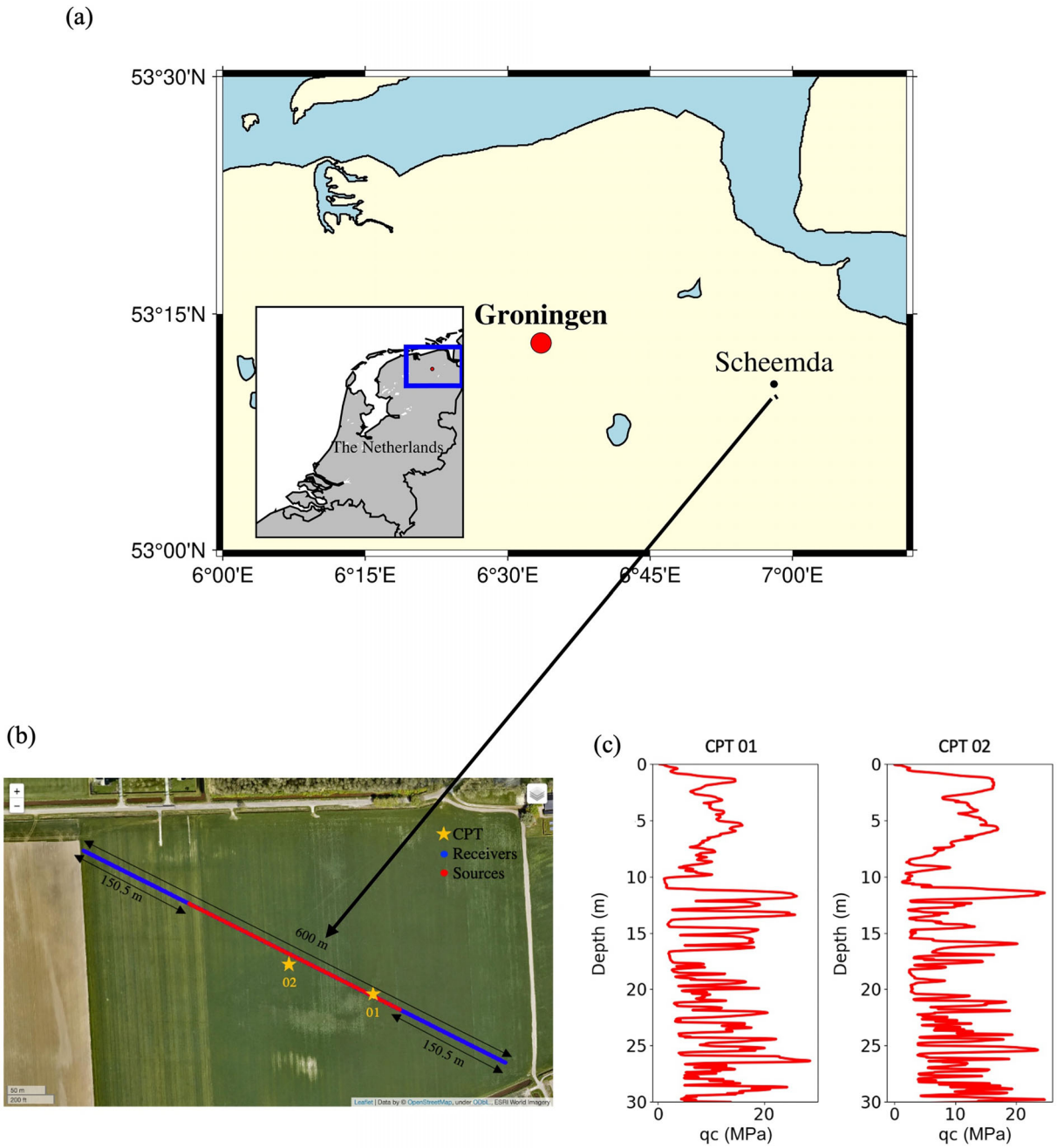


**Figure 2** | (a) Location of the site and (b) the geometry of the reflection line. In (b), the red circles represent active sources, the blue circles represent receivers and the orange stars represent the locations of two cone penetration tests (CPTs). (c) Cone-tip resistance (qc) was measured at the two CPT locations.

## 2.2 | Over- and Underburden Removal

The isolated responses of the target layer are retrieved through a two-step procedure. First, the overburden is removed, followed by the underburden removal. As introduced above, the medium is divided into three units: $\langle a \rangle$ the overburden, $\langle b \rangle$ the target layer, and $\langle c \rangle$ the underburden, as shown in Figure 1. In the first step, for the overburden removal, a focal level is selected between the overburden $\langle a \rangle$ and the target zone $\langle b \rangle$, and Equations (3) and (4) are employed to determine the extrapolated Green's functions using the original reflection responses ($R_{abc}$). For the overburden removal, the retrieved extrapolated Green's functions are employed to retrieve the reflection response isolated from the overburden interferences using

$$U^{-,+}_{a|bc}(\mathbf{x}_R, \mathbf{x}'_S, t) = -\int_{S_0} U^{-,-}_{a|bc}(\mathbf{x}_R, \mathbf{x}'_R, t) * R_{bc}(\mathbf{x}'_R, \mathbf{x}'_S, t) d\mathbf{x}'_R, \quad (5)$$

where $U^{-,\pm}_{a|bc}$ represents the extrapolated Green's functions (Wapenaar et al. 2021; van IJsseldijk 2023). The vertical line in the subscript indicates the location of the focal level, that is, between the overburden $\langle a \rangle$ and the target zone and underburden $\langle bc \rangle$. Using Equation (5), the reflection response $R_{bc}$ is retrieved employing SI by MDD. The retrieved $R_{bc}$ contains all primary and

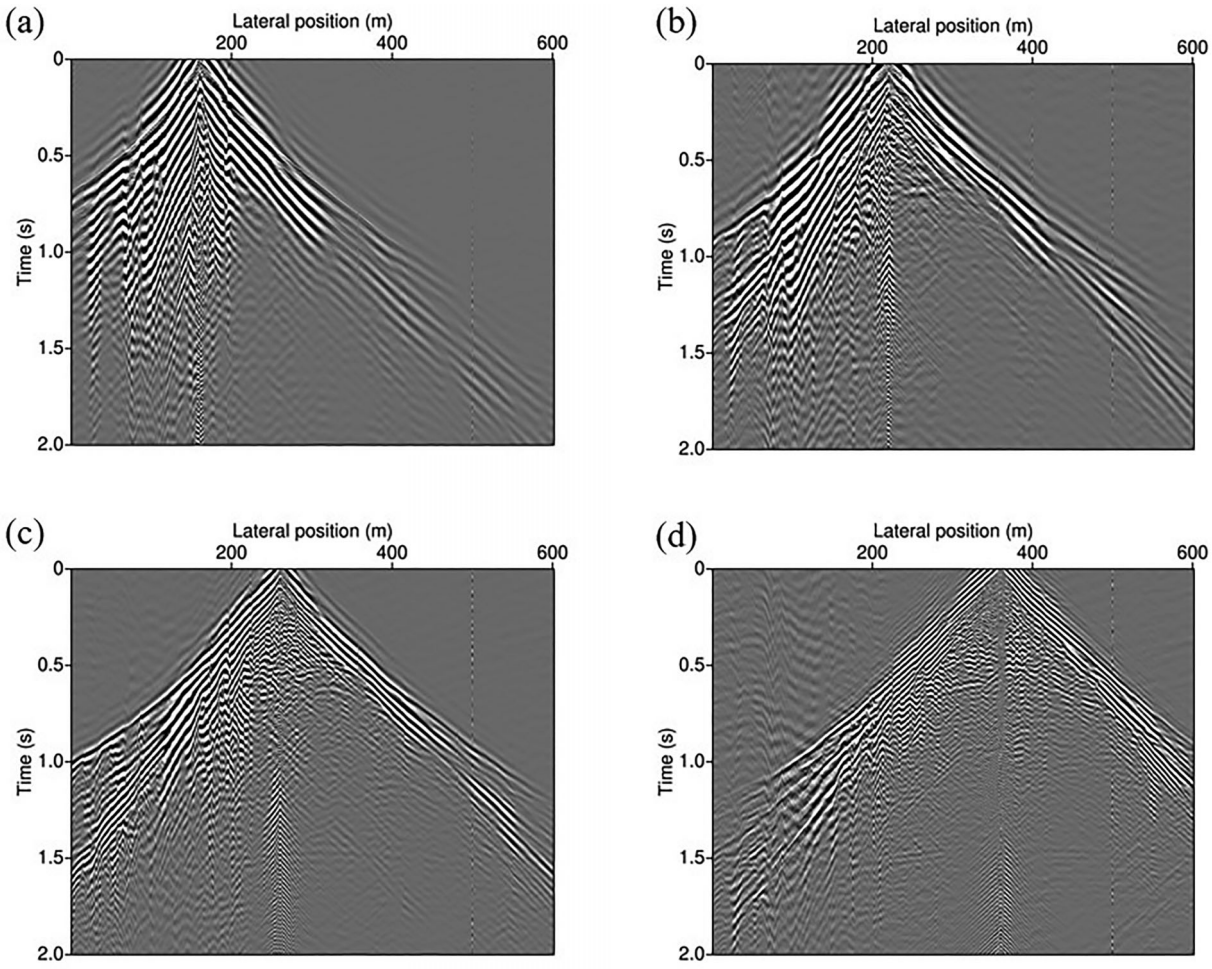


**Figure 3** | Raw common-source gathers for active sources at lateral positions: (a) 165.5 m, (b) 220.5 m, (c) 260.5 m and (d) 360.5 m.

**Table 1** | Acquisition parameters.

| Parameter | Value |
|---|---|
| Number of source positions | 151 |
| Source spacing | 2.0 m |
| First source position | 150.5 |
| Last source position | 450.5 |
| Number of receiver positions per source | 601 |
| Receiver spacing | 1.0 m |
| First receiver position | 0 m |
| Frequency range of the sweep | 8-250 Hz |

multiple reflections from the target zone $\langle b \rangle$ and underburden $\langle c \rangle$, but it is devoid of overburden interactions from $\langle a \rangle$. Additionally, the coordinates $\mathbf{x}'_R$ and $\mathbf{x}'_S$ are situated at the surface, owing to the utilisation of the extrapolated Green's functions (van IJsseldijk et al. 2023).

For the next step, which is the underburden removal, this new reflection response ($R_{bc}$) can be utilised to retrieve the extrapolated focusing functions for a focal level between the target zone $\langle b \rangle$ and the underburden $\langle c \rangle$ using Equations (3) and (4) (Wapenaar and Staring 2018; van IJsseldijk et al. 2024). Then, to remove the underburden, we employ the following relation between the retrieved extrapolated focusing functions and the reflection response of the target ($R_b$):

$$v^-_{b|c}(\mathbf{x}_R, \mathbf{x}'_S, t) = \int_{S_0} v^+_{b|c}(\mathbf{x}_R, \mathbf{x}'_R, t) * R_b(\mathbf{x}'_R, \mathbf{x}'_S, t) d\mathbf{x}'_R. \quad (6)$$

The subscript $b|c$ indicates that the extrapolated focusing functions have been obtained from the reflection response without overburden interaction, utilising a focal depth between the target zone $\langle b \rangle$ and underburden $\langle c \rangle$. Once again, the isolated reflection response ($R_b$) can be retrieved from this equation through SI by MDD. Effectively, the target-zone response has now been isolated; the isolated response consists of the reflections (primaries and multiples) from inside the target zone only (van IJsseldijk et al. 2024). Figure 1 shows this two-step procedure for removing the overburden and underburden using the Marchenko-based isolation.

## 3 | Seismic Data Acquisition

In the summer of 2022, seismic reflection data were acquired along a line close to the town of Scheemda in the Groningen

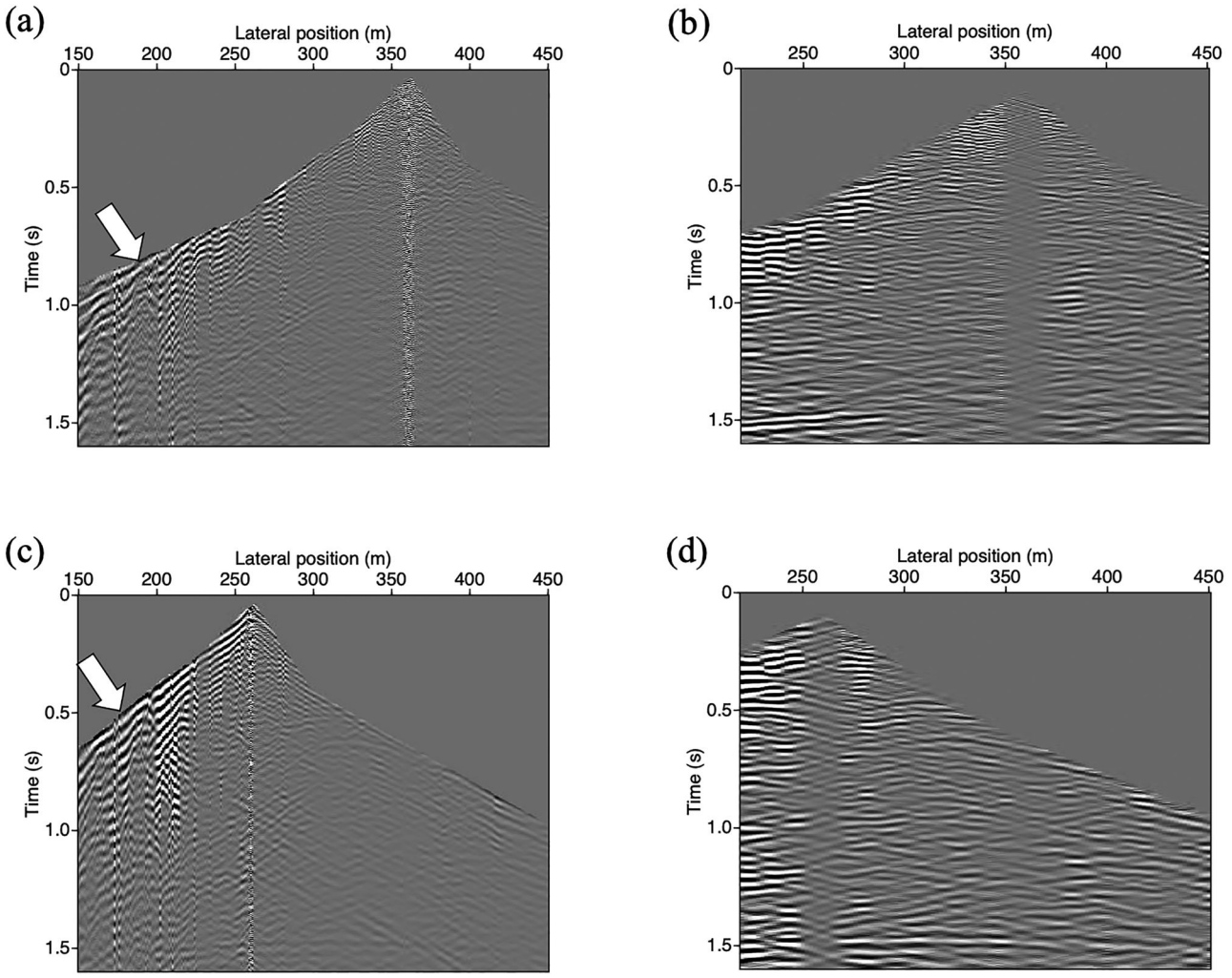


**Figure 4** | Common-source gathers: (a) after the initial pre-processing steps and (b) after the final pre-processing steps for a source at a lateral position at 360.5 m. (c) and (d) are the same as (a) and (b), respectively, but for a source at 260.5 m. The white arrows indicate strong surface waves at the receiver positions at 150–220 m.

province of the Netherlands. Figure 2a and 2b shows the location of the site and the geometry of the reflection line, respectively, and Figure 2c shows two examples of CPT data from this site.

We employed an electric seismic vibrator (Noorlandt et al. 2015) as a source with a spacing of 2.0 m (the red circles in Figure 2b), and 601 three-component geophone nodes as receivers (the blue circles in Figure 2b), with a spacing of 1.0 m. The acquisition parameters are summarised in Table 1.

This dataset was acquired primarily for use with the Marchenko method, so specific requirements were taken into account – for example, using densely and regularly spaced receivers and placing sources close to the receivers (0.5 m spacing). Additionally, we made use of the vibrator in the S-wave mode, oriented in the crossline direction. To apply the Marchenko method, we then use the data recorded by the crossline horizontal component of the geophones. Because of the orientation of the sources and the receivers, and assuming no scattering from the crossline direction, the SH-waves we record are generally decoupled from the compressional and vertically polarised S-waves. This makes the dataset more convenient for applying the Marchenko method.

Four examples of common-source gathers at different source positions are shown in Figure 3.

## 4 | Data Pre-Processing

The raw seismic reflection data cannot directly be used by the Marchenko method because when the method uses these data, it does not converge to a solution, likely due to amplitude errors in the recorded data (Thorbecke et al. 2017). As a first data pre-processing step, we apply source-signature deconvolution to obtain high-resolution zero-phase reflection responses as input, which is crucial for the Marchenko method. We use the designed source parameters as sent to the vibrator for a source-signature deconvolution.

In seismic land surveys with sources and receivers at the surface, the surface waves are most of the time dominant and they mask the reflections. This is also the case in our data. To eliminate surface waves, we apply surgical muting in the time domain and then employ bandpass filtering between 30 and 100 Hz based on the power spectrum of the common-source

gathers. To avoid any trace distortion, we chose not to use frequency–wavenumber filtering.

The subsequent steps involved in preparing the reflection data for applying the Marchenko method represent amplitude corrections. First, we correct the amplitudes for recording a two-dimensional (2D) line in a three-dimensional (3D) world. The effects of having geometric spreading in a 3D world while applying a 2D Marchenko scheme are corrected by applying a time-dependent gain to the data. This gain is approximately equal to $\sqrt{t}$ (Helgesen and Kolb 1993; Brackenhoff et al. 2019). After that, we correct for absorption effects and for an overall amplitude mismatch that, for example, is related to the source signature. This is achieved by minimising a cost function as described in Brackenhoff (2016). Different gains and linear factors are considered in order to find an optimal correction factor (van IJsseldijk 2023).

The Marchenko-method application uses the same number of sources and receivers; however, our survey has more receivers positions than source positions. Therefore, we constrain our receivers to the extent and number of the sources, that is, to the range 150–450 m with 2.0 m spacing.

Figure 4a,c shows two common-source gathers after the application of the above-mentioned pre-processing steps. In these figures, it is evident that some pronounced surface waves persist at receivers positioned laterally between 150 and 220 m, as indicated by the white arrows. Additionally, when comparing the common-source gathers shown in Figure 3, variations in the frequency content of the surface waves become apparent for sources located at lateral positions 150–220 m. This variation may occur due to local scattering in the shallow subsurface. Therefore, we further limit our sources and receivers to the range 220–450 m. Moreover, we see from the preprocessed gathers that the traces closest to the source location appear to have too strong amplitudes, that is, they are strongly influenced by the source (near-field effects), which would result in difficulties during the inversion. Thus, we mute the 20 nearest traces around each source location, and then finally we apply a bandpass filter between 30 and 100 Hz. Figure 4b and 4d shows the common-source gathers from Figures 4a and 4c, respectively, after all pre-processing steps, showcasing enhancement in the visibility of the reflections. Additionally, we select only the earliest 1.6 s, as our primary focus lies in improving reflections up to this time. These processed data are then utilised as input for the Marchenko-based isolation technique.

As discussed in Section 2, we also require a smooth velocity model of the subsurface below the acquisition line to separate the focusing functions from the Green's functions by estimating the two-way travel time between the surface and the focal depth. We obtain a one-dimensional (1D) smooth velocity model by standard normal moveout (NMO) analysis applied to CMP gathers. Figure 5 shows the estimated smooth 1D velocity model.

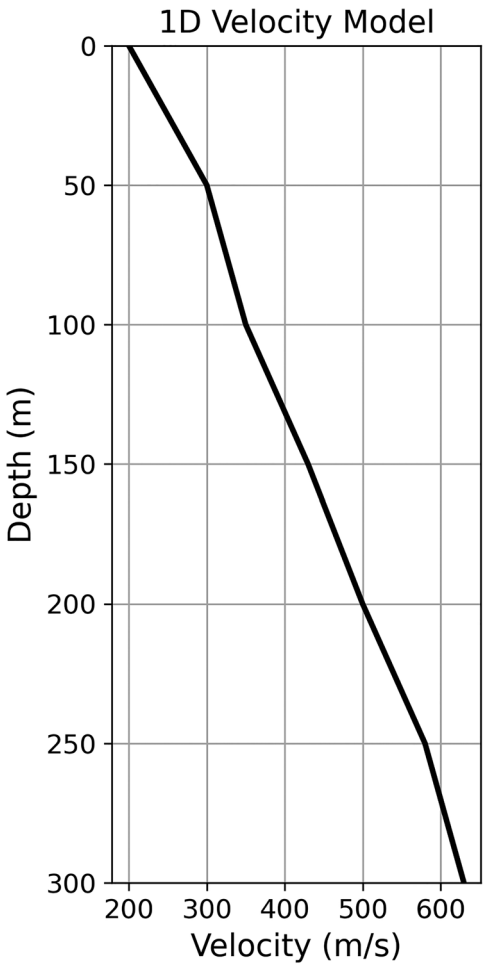


**Figure 5** | A smooth 1D SH-velocity model obtained from normal-moveout analysis on common-midpoint gathers.

## 5 | The Results From Marchenko-Based Isolation

After completing the pre-processing steps, we employ the processed reflection data to extract the Green's functions and isolate the responses of the target region, using the Marchenko-based isolation technique with one iteration. To account for both overburden and underburden effects, we employ the two-step procedure explained in Section 2. In the first step, we eliminate the overburden effect by choosing a focal depth of 30 m. Subsequently, using the results obtained from the first step, we eliminate the underburden effect by choosing a focal depth of 270 m. This two-step approach leaves the isolated response of the target region between 30 and 270 m depth. Figure 6 shows an overview of the data pre-processing steps and the process to isolate the target response.

Figure 7 shows two common-source gathers before and after the Marchenko-based isolation. By comparing the common-source gathers before (Figure 7a,c) and after the Marchenko-based isolation (Figure 7b,d), it is evident that the resolution and clarity of some reflections are enhanced, as indicated by the cyan, yellow and red arrows.

To facilitate a further comparison of the results, we perform NMO correction and stacking using CMP gathers for both the original and the Marchenko-isolated responses. We use different constant velocities, an average velocity of the target region and the time-varying NMO velocity for the NMO correction and stacking. By comparison, the constant velocity of 350 m/s leads to improved

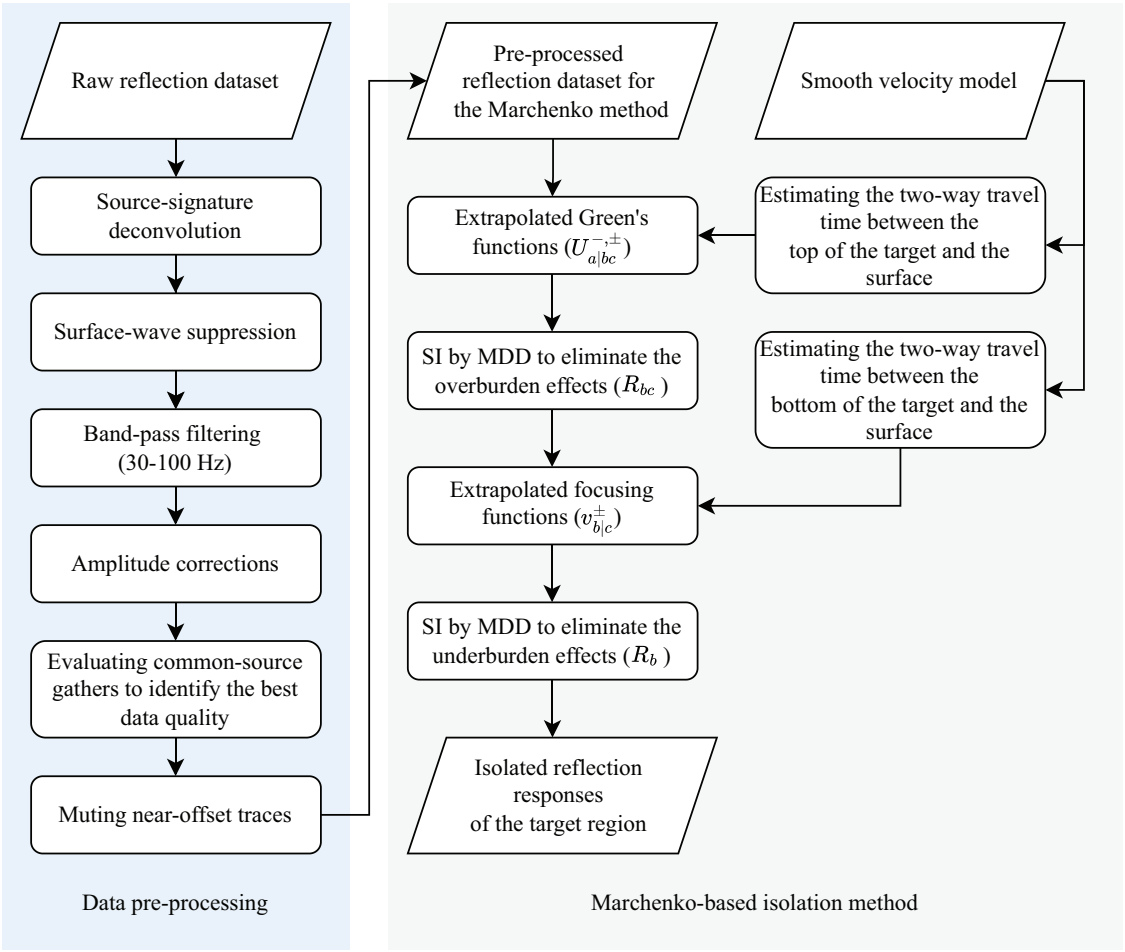


**Figure 6** | Flowchart showing data pre-processing steps and the Marchenko-based isolation method.

results regarding clear reflectors. We then apply an automatic gain control with a time-window length of 400 ms to aid the visual comparison. The stacked sections for both the original and the Marchenko-based isolated responses are shown in Figure 8.

The stacked section obtained from the Marchenko-based isolated responses in Figure 8b is cleaner than the stacked section using the original reflection response (with the same spatial extent) in Figure 8a. Moreover, the Marchenko-isolated stacked section exhibits more continuity, helping in interpreting the data better. The events marked with cyan, yellow, orange and red arrows indicate improvements in the stacked section in the case of the Marchenko-based isolation. Note that the orange arrow in Figure 8a may not point to a particularly clear feature. However, we used the same arrow in this figure as in Figure 8b, which are the results of the Marchenko method. The arrow draws attention to an event that the Marchenko method has helped unravel from beneath the 'noise' of internal multiples. Maintaining consistency in the arrow placement ensures a direct comparison of the same features between the original reflection dataset and the Marchenko method results.

To assess the individual effects of the overburden and underburden on the final result, we perform overburden and underburden removal separately. Figure 8c shows the stacked section after overburden removal, while Figure 8d shows the stacked section after underburden removal. By comparing Figure 8c,d with Figure 8b, it becomes evident that most of the interaction originates from the overburden. The removal of the underburden does not improve the interpretability of the stacked sections, as enhancements are expected for arrivals after 1.42 s for a focal depth of 270 m using the estimated average velocity of 380 m/s from the smooth velocity model. This is likely due to small velocity variation in the underburden and attenuation of the reflected S-waves from the deeper layers. Additionally, the noise observed in Figure 8d may be attributed to the influence of the overburden.

To better visualise the shallow part of the section, we further zoom in from 0.6 to 1.0 s (see Figure 9). The geology in the top 30 m at this site, known from the cone-tip resistance (qc) measured at the two CPT locations (Figure 2c), comprises alternating clay and sand layers that contribute to the generation of internal multiples in this shallow section. Comparing the stacked section before Marchenko-based isolation in Figure 9a with the stacked section after Marchenko-based isolation in Figure 9b suggests a potential elimination of such internal multiples originating from the overburden down to 30 m in our case. Similar to the deeper reflectors, these shallow reflectors appear clearer and more continuous, as indicated by the colour-coded arrows.

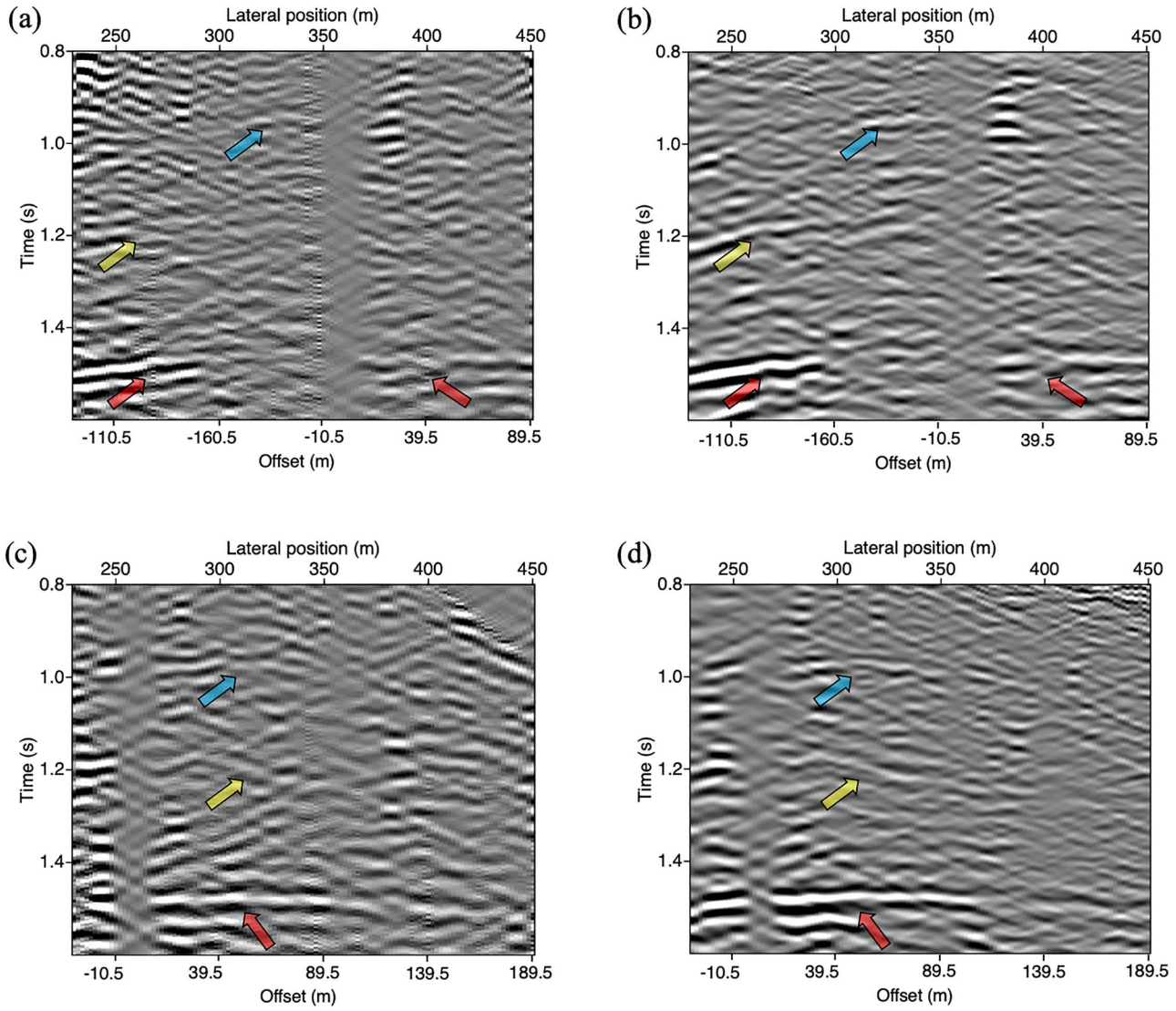


**Figure 7** | A common-source gather for a source at a lateral position at 360.5 m (a) before and (b) after the Marchenko-based isolation. (c) and (d) are the same as (a) and (b), respectively, but for a source at 260.5 m. The cyan, yellow and red arrows indicate reflections. The same bandpass filtering between 30 and 100 Hz was applied for better comparison.

## 6 | Discussion

As demonstrated in the preceding section, from the comparison of the common-source gathers and the unmigrated stacked sections (Figures 7–9), the results of the Marchenko method show an improved signal-to-noise ratio, providing a clearer and more accurate image of the target zone compared to the original reflection responses. This improvement arises because, by using the Marchenko isolation method, we successfully removed the effects of the overburden and underburden. Particularly, in our dataset, we removed the effects of the first 30 m of this site, which consists of alternating layers (known from the CPT profile) capable of generating strong internal multiples. These multiples interfere with the subsurface response of the target layers. For example, the orange arrow in Figure 8 indicates a reflection event that is clearly interpretable after the Marchenko isolation, while it is not interpretable in the conventional stacked section (obtained by careful processing). This is critically important for future studies because it allows us to study changes within the target layers over time without any effects from the overburden and underburden, as shown by Van IJsseldijk et al. (2024) for time-lapse monitoring using a marine dataset of the Troll field in Norway. Even though we observe clear improvements in the reflection-data resolution and clarity, there are potential options for further enhancement in future studies and some extra measures to address the shortcomings of the Marchenko method.

First, the method is intentionally designed to minimise reliance on a priori information, utilising only a smoothed version of the velocity model and the recorded reflection responses. We obtained the 1D smooth velocity model using the standard NMO analysis applied to CMP) gathers. In general, it is recommended to use a smooth macro velocity model that represents the medium, including potential lateral velocity variations.

The Marchenko method relies on seismic reflection data, which, however, cannot be used directly. Therefore, careful pre-processing (see Figure 6) is essential for its practical application

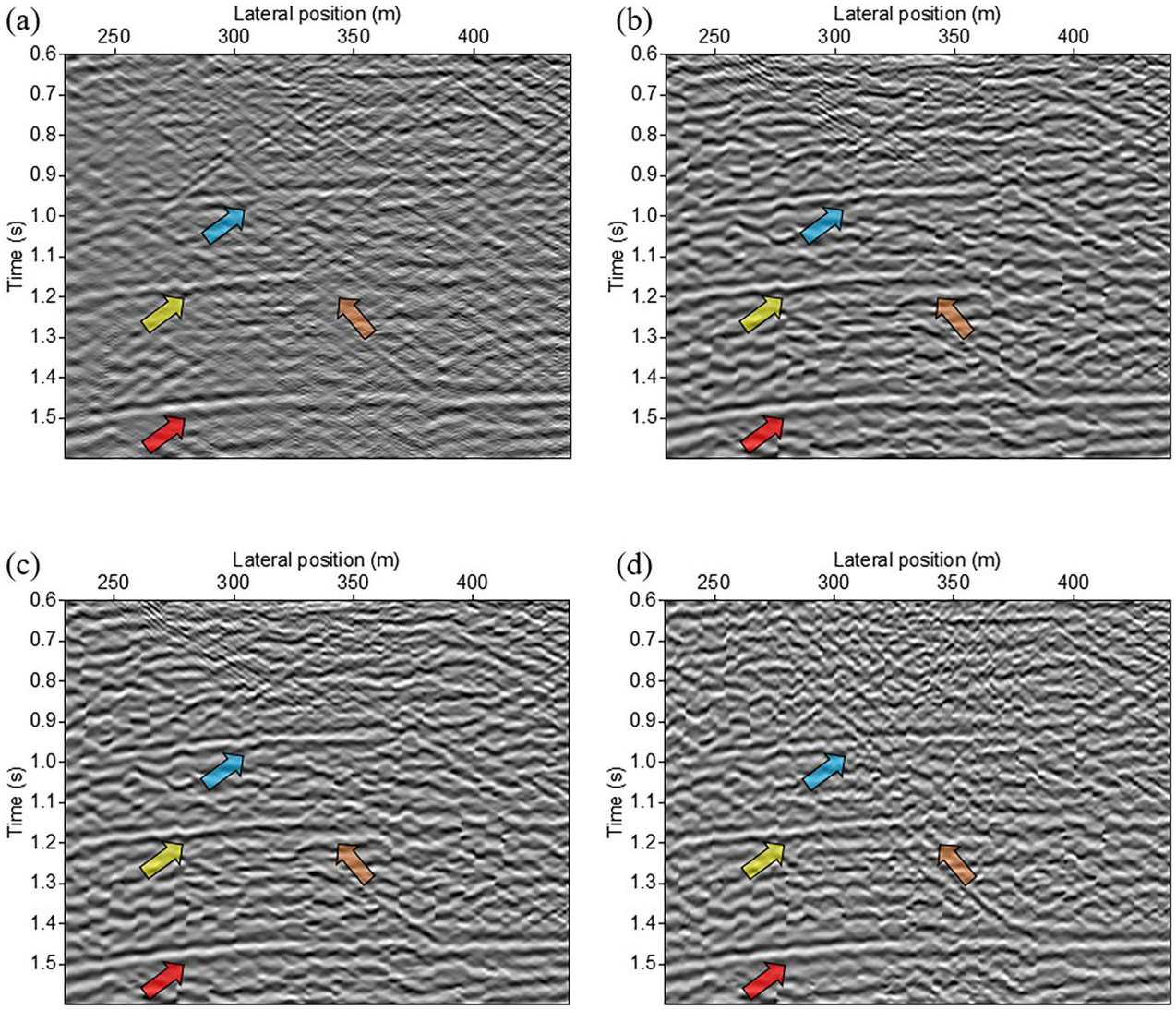


**Figure 8** | The stacked sections obtained from (a) the original reflection response and (b) the reflection response after the Marchenko-based isolation for overburden and underburden removal, (c) same as (b) but after only overburden removal, (d) same as (b) but after only underburden removal. The colour-coded arrows indicate reflections.

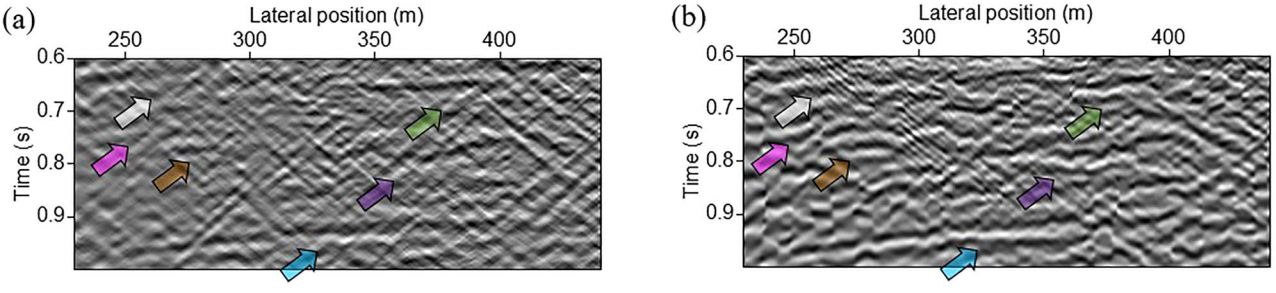


**Figure 9** | Stacked sections, zoomed in between 0.6 and 1.0 s, obtained using (a) the original reflection response and (b) the reflection response after Marchenko-based isolation for overburden and underburden removal.

to field datasets. The Marchenko method has been successfully applied to field data (Ravasi et al. 2016; Jia et al. 2018; Staring et al. 2018; Mildner et al. 2019; Zhang and Slob 2020) through a series of pre-processing steps, primarily source-signature deconvolution and amplitude corrections. Some of these steps, such as the elimination of surface-related multiples, can be dataset-specific, for example, for marine datasets. In this study, we introduced additional steps specifically designed for our land seismic dataset. The first one is surface-wave suppression. Surface waves were suppressed using surgical muting in the time domain and

frequency filtering. It may also be beneficial to explore other techniques, such as seismic interferometry, for surface-wave suppression, as demonstrated in prior studies (Liu et al. 2018; Balestrini et al. 2020; Shirmohammadi 2024). Second, we applied muting of specific traces to remove excessive amplitudes. The goal of all these pre-processing steps was to produce clear reflection datasets for the accurate application of the Marchenko method. Depending on the characteristics of different datasets, additional survey-specific pre-processing steps may be required to optimize the data quality. Nevertheless, a pre-processing sequence should produce clearer reflection data. As long as the quality of the obtained reflection data is good, the result of the Marchenko redatuming should not depend significantly on the chosen pre-processing sequence. If the quality is below par, the Marchenko redatuming might not converge.

One of the constraints of the Marchenko method is its requirement for well-sampled and co-located sources and receivers. While our dataset was well-sampled, the sources were not precisely co-located with the receivers but were positioned 0.5 m away. However, this is acceptable given the expected minimum wavelength of 2 m, as the 0.5 m distance is still less than the minimum wavelength. For a dataset with irregular or imperfect sampling, van IJsseldijk and Wapenaar (2020) demonstrated that the iterative Marchenko approach can be adapted to work with irregularly sampled data by using point-spread functions to recreate results as if they were acquired under perfect geometric conditions. Moreover, the Marchenko method can effectively handle mild variations in topography; however, strongly variable topography will cause problems. This is not a limitation specific to the Marchenko method, as conventional reflection-data processing faces similar challenges under such conditions.

One significant challenge in applying the Marchenko method to field data lies in the amplitude-scaling requirements on the reflection data. We tried to overcome amplitude mismatches by applying three gain factors for geometrical spreading, absorption effects and an overall scaling. However, additional errors may arise from wavefield damping and incomplete source-signature removal. Several attempts have been made to improve amplitude scaling. For example, Staring et al. (2021) proposed a pre-processing approach that determines a scaling factor by matching predicted surface-related multiples with those observed in the data. This method requires the presence of surface-related multiples, making it particularly suitable for surveys in shallow water environments. In another study, Dukalski and Reinicke (2022) introduced a more accurate correction for geometrical spreading, though it is currently limited to 1.5D media (van IJsseldijk 2023). Because amplitude-scaling issues depend on subsurface geology, a universal correction method may not be feasible. Further research is needed to better understand and address these scaling errors for land data and SH-waves in particular.

In this study, we applied the Marchenko-based isolation technique by selecting focal depths at 30 and 270 m. We observed that the most significant improvement comes from the overburden removal. However, choosing different focal depths with smaller intervals and focusing on the improvement of specific reflections could be valuable in future studies.

Finally, the comparison of the common-source gathers and the unmigrated time sections, using a constant velocity for stacking, provided a good basis for our dataset, but we propose the application of a more realistic velocity analysis followed by migration. This additional step could contribute to a more comprehensive understanding and improvement of the Marchenko-based isolation technique.

## 7 | Conclusion

We showed the result of applying the Marchenko-based isolation technique to SH-wave land seismic data that we acquired in the Groningen province, the Netherlands. Land seismic data are known for dominant surface waves and a low signal-to-noise ratio. Therefore, it is challenging to use the Marchenko method on land-seismic data, as the method ideally requires high-quality data. After careful implementation of surface-wave suppression, selection of the same spatial extent of sources and receivers and the scaling-factor corrections as pre-processing steps, we retrieved the extrapolated Green's functions, focusing functions and the isolated target responses after the combined removal of the overburden and the underburden.

We showed that the resulting stacked section has an improved signal-to-noise ratio, providing a better image of the target zone compared to the stacked original reflection response. Our results open the door for future applications of the Marchenko method to land seismic datasets, particularly for time-lapse monitoring of the deeper structures, for example, for $CO_2$ and $H_2$ storage or shallow applications such as monitoring waste management and changes in the water table or other hydrological parameters.


### Acknowledgements

We acknowledge the use of computational resources provided by the DelftBlue supercomputer at the Delft High Performance Computing Centre (https://www.tudelft.nl/dhpc) and thank Seismic Mechatronics for allowing us to use their vibrator source during fieldwork (https://seismic-mechatronics.com/).


### Data Availability Statement

The field reflection dataset used in this study is available in the 4TU.ResearchData repository at https://doi.org/10.4121/a8553b7e-82ae-4e9b-bc54-2a6b9ca6063c. Codes associated with this study are available and can be accessed via the following URL: https://gitlab.com/geophysicsdelft/OpenSource in the 'vmar' folder. More explanation can be found in van IJsseldijk et al. (2023).

### References


Bakulin, A., and R. Calvert. 2006. "The Virtual Source Method: Theory and Case Study." *Geophysics* 71, no. 4: SI139–SI150. https://doi.org/10.1190/1.2216190

Balestrini, F., D. Draganov, A. Malehmir, P. Marsden, and R. Ghose. 2020. "Improved Target Illumination at Ludvika Mines of Sweden Through Seismic-Interferometric Surface-Wave Suppression." *Geophysical Prospecting* 68, no. 1: 200–213. https://doi.org/10.1111/1365-2478.12890

Brackenhoff, J. 2016. Rescaling of Incorrect Source Strength Using Marchenko Redatuming. M.Sc. thesis, Delft University of Technology. http://resolver.tudelft.nl/uuid:0f0ce3d0-088f-4306-b884-12054c39d5da.

Brackenhoff, J., J. Thorbecke, and K. Wapenaar. 2019. "Virtual Sources and Receivers in the Real Earth: Considerations for Practical Applications." *Journal of Geophysical Research: Solid Earth* 124, no. 11: 11802–11821. https://doi.org/10.1029/2019JB018485

Broggini, F., K. Wapenaar, J. van der Neut, and R. Snieder. 2014. "Data-Driven Green's Function Retrieval and Application to Imaging With Multidimensional Deconvolution." *Journal of Geophysical Research: Solid Earth* 119, no. 1: 425–441. https://doi.org/10.1002/2013JB010544

Dukalski, M., and C. Reinicke. 2022. Marchenko Multiple Elimination Using Conventional vs Advanced 3-D to 2-D Conversion on Marine Data. In the 83rd EAGE Conference and Exhibition 2022 2022, no. 1: 1–5. European Association of Geoscientists & Engineers. https://doi.org/10.3997/2214-4609.202210182

Helgesen, J., and P. Kolb. 1993. "Multi-Offset Acoustic Inversion of a Laterally Invariant Medium: Application to Real Data." *Geophysical Prospecting* 41, no. 5: 517–533. https://doi.org/10.1111/j.1365-2478.1993.tb00868.x

Jia, X., A. Guitton, and R. Snieder. 2018. "A Practical Implementation of Subsalt Marchenko Imaging With a Gulf of Mexico Data Set." *Geophysics* 83, no. 5: S409–S419. https://doi.org/10.1190/geo2017-0646.1

Kruiver, P. P., E. Dedem van, R. Romijn, G.de Lange, M. Korff, J. Stafleu, J. L. Gunnink, A. Rodriguez-Marek, J. J. Bommer, J. van Elk, and D. Doornhof. 2017. "An Integrated Shear-Wave Velocity Model for the Groningen Gas Field, The Netherlands." *Bulletin of Earthquake Engineering* 15: 3555–3580. http://link.springer.com/10.1007/s10518-017-0105-y

Liu, J., D. Draganov, and R. Ghose. 2018. "Seismic Interferometry Facilitating the Imaging of Shallow Shear-Wave Reflections Hidden Beneath Surface Waves." *Near Surface Geophysics* 16, no. 3: 372–382. https://doi.org/10.3997/1873-0604.2018013

Malcolm, A. E., M. V. de Hoop, and H. Calandra. 2007. "Identification of Image Artifacts From Internal Multiples." *Geophysics* 72, no. 2: S123–S132. https://doi.org/10.1190/1.2434780

Meles, G. A., K. Wapenaar, and A. Curtis. 2016. "Reconstructing the Primary Reflections in Seismic Data by Marchenko Redatuming and Convolutional Interferometry."*Geophysics* 81, no. 2: Q15–Q26. https://doi.org/10.1190/geo2015-0377.1

Mildner, C., F. Broggini, C. A. da Costa Filho, and J. O. Robertsson. 2019. "Source Wavelet Correction for Practical Marchenko Imaging: A Sub-Salt Field-Data Example From the Gulf of Mexico." *Geophysical Prospecting* 67, no. 8: 2085–2103. https://doi.org/10.1111/1365-2478.12822

Mulder, W.A. 2005. "Rigorous Redatuming." *Geophysical Journal International* 161, no. 2: 401–415. https://doi.org/10.1111/j.1365-246X.2005.02615.x

Muntendam-Bos, A. G., G. Hoedeman, K. Polychronopoulou, D. Draganov, C. Weemstra, W. van der Zee, R. R. Bakker, and H. Roest. 2022. "An Overview of Induced Seismicity in the Netherlands." *Geologie en Mijnbouw/Netherlands Journal of Geosciences* 101, no. 2: 1–20. https://doi.org/10.1017/njg.2021.14

Noorlandt, R., G. Drijkoningen, J. Dams, and R. Jenneskens. 2015. "A Seismic Vertical Vibrator Driven by Linear Synchronous Motors." *Geophysics* 80, no. 2: EN57–EN67. https://doi.org/10.1190/GEO2014-0295.1

Ravasi, M., I. Vasconcelos, A. Kritski, A. Curtis, C. A. da Costa Filho, and G. A. Meles. 2016. "Target-Oriented Marchenko Imaging of a North Sea Field." *Geophysical Journal International* 205, no. 1: 99–104. https://doi.org/10.1093/gji/ggv528

Reinicke, C., M. Dukalski, and K. Wapenaar. 2020. "Comparison of Monotonicity Challenges Encountered by the Inverse Scattering Series and the Marchenko Demultiple Method for Elastic Waves." *Geophysics* 85, no. 5: Q11–Q26. https://doi.org/10.1190/geo2019-0674.1

Schuster, G. T., J. Yu, J. Sheng, and J. Rickett. 2004. "Interferometric/Daylight Seismic Imaging." *Geophysical Journal International* 157, no. 2: 838–852. https://doi.org/10.1111/j.1365-246X.2004.02251.x

Shirmohammadi, F. 2024. "Layer-Specific Imaging and Monitoring Using Seismic Interferometry and the Marchenko Method." Ph.D. thesis, Delft University of Technology. http://resolver.tudelft.nl/uuid:425a6761-cb96-4326-aeb8-e2a312588765.

Shirmohammadi, F., D. Draganov, M. R. Hatami, and C. Weemstra. 2021. "Application of Seismic Interferometry by Multidimensional Deconvolution to Earthquake Data Recorded in Malargüe, Argentina." *Remote Sensing* 13, no. 23: 4818. https://doi.org/10.3390/rs13234818

Slob, E., K. Wapenaar, F. Broggini, and R. Snieder. 2014. "Seismic Reflector Imaging Using Internal Multiples With Marchenko-Type Equations." *Geophysics* 79, no. 2: S63–S76. https://doi.org/10.1190/GEO2013-0095.1

Staring, M., M. Dukalski, M. Belonosov, R. H. Baardman, J. Yoo, R. F. Hegge, R. van Borselen, and K. Wapenaar. 2021. "Robust Estimation of Primaries by Sparse Inversion and Marchenko Equation-Based Workflow for Multiple Suppression in the Case of a Shallow Water Layer and a Complex Overburden: A 2D Case Study in the Arabian Gulf." *Geophysics* 86, no. 2: Q15–Q25. https://doi.org/10.1190/geo2020-0204.1

Staring, M., R. Pereira, H. Douma, J. van der Neut, and K. Wapenaar. 2018. "Source-Receiver Marchenko Redatuming on Field Data Using an Adaptive Double-Focusing Method." *Geophysics* 83, no. 6: S579–S590. https://doi.org/10.1190/geo2017-0796.1

Thorbecke, J., E. Slob, J. Brackenhoff, J.van der Neut, and K. Wapenaar. 2017. "Implementation of the Marchenko Method." *Geophysics* 82: WB29–WB45. https://doi.org/10.1190/GEO2017-0108.1

van der Neut, J., J. Thorbecke, K. Wapenaar, and E. Slob. 2015. Inversion of the Multidimensional Marchenko Equation. In the 77th EAGE Conference and Exhibition 2015, June 2015, Volume 2015, pp. 1–5. https://doi.org/10.3997/2214-4609.201412939

van der Neut, J., and K. Wapenaar. 2016. "Adaptive Overburden Elimination With the Multidimensional Marchenko Equation." *Geophysics* 81, no. 5: T265–T284. https://doi.org/10.1190/GEO2016-0024.1

van IJsseldijk, J. 2023. Time-Lapse Monitoring With Virtual Seismology. Ph.D. thesis, Delft University of Technology. https://doi.org/10.4233/uuid:98b24420-219b-438e-a28c-4b12e5f450e6.

van IJsseldijk, J., J. Brackenhoff, J. Thorbecke, and K. Wapenaar. 2024. "Time-Lapse Applications of the Marchenko Method on the Troll Field." *Geophysical Prospecting* 72: 1026–1036. https://doi.org/10.1111/1365-2478.13463

van IJsseldijk, J., J. van der Neut, J. Thorbecke, and K. Wapenaar. 2023. "Extracting Small Time-Lapse Traveltime Changes in a Reservoir Using Primaries and Internal Multiples After Marchenko-Based Target Zone Isolation." *Geophysics* 88, no. 2: R135–R143. https://doi.org/10.1190/geo2022-0227.1

van IJsseldijk, J., J. van der Neut, J. Thorbecke, and K. Wapenaar. 2023. "Extracting Small Time-Lapse Traveltime Changes in a Reservoir Using Primaries and Internal Multiples After Marchenko-Based Target Zone Isolation." *Geophysics* 88, no. 2: R135–R143.

van IJsseldijk, J., and K. Wapenaar. 2020. "Adaptation of the Iterative Marchenko Scheme for Imperfectly Sampled Data." *Geophysical Journal International* 224, no. 1: 326–336. https://doi.org/10.1093/gji/ggaa463

Wapenaar, K., J. Brackenhoff, M. Dukalski, G. Meles, C. Reinicke, E. Slob, M. Staring, J. Thorbecke, J. van der Neut, and L. Zhang. 2021. "Marchenko Redatuming, Imaging, and Multiple Elimination and Their Mutual Relations." *Geophysics* 86, no. 5: WC117–WC140. https://doi.org/10.1190/geo2020-0854.1

Wapenaar, K., and M. Staring. 2018. "Marchenko-Based Target Replacement, Accounting for All Orders of Multiple Reflections." *Journal of Geophysical Research: Solid Earth* 123, no. 6: 4942–4964. https://doi.org/10.1029/2017JB015208

Wapenaar, K., J. Thorbecke, J. van der Neut, F. Broggini, E. Slob, and R. Snieder. 2014a. "Marchenko Imaging." *Geophysics* 79, no. 3: WA39–WA57. https://doi.org/10.1190/GEO2013-0302.1

Wapenaar, K., J. Thorbecke, J. van der Neut, F. Broggini, E. Slob, and R. Snieder. 2014b. "Green's Function Retrieval From Reflection Data, in Absence of a Receiver at the Virtual Source Position." *The Journal of the Acoustical Society of America* 135, no. 5: 2847–2861. https://doi.org/10.1121/1.4869083

Wapenaar, K., and J. van IJsseldijk. 2021. Employing Internal Multiples in Time-Lapse Seismic Monitoring, Using the Marchenko Method. In the 82nd EAGE Conference and Exhibition 2021, pp. 1–5. European Association of Geoscientists & Engineers. https://doi.org/10.3997/2214-4609.202011576

Zhang, L., and E. Slob. 2020. "A Field Data Example of Marchenko Multiple Elimination." *Geophysics* 85, no. 2: S65–S70. https://doi.org/10.1190/geo2019-0327.1